Evolutionary Tracking Algorithm Based on Combined Received Signal Strength and Angle of Arrival Measurements in Wireless Sensor Networks

Lismer Andres Caceres Najarro, Iickho Song, *Fellow, IEEE*, Slavisa Tomic, Muhammad Salman, Youngtae Noh, *Member, IEEE*, and Kiseon Kim, *Life Senior Member, IEEE*

***Abstract*—This article addresses the target tracking problem based on the received signal strength (RSS) and angle of arrival (AOA) in wireless sensor networks (WSNs). The tracking problem is formulated in the framework of the maximum a posteriori (MAP), in which the prior knowledge of moving target nodes (TNs) is exploited. Due to the fact that the cost function of the tracking problem is highly nonlinear and nonconvex, most of the existing algorithms tend to approximate and relax the cost function. As a result, the tracking accuracy is usually compromised. In this article, we propose a tracking algorithm based on evolutionary techniques that do not require an approximation of the cost function, resulting in a considerable improvement in tracking accuracy. The proposed tracking algorithm is compared with state-of-the-art algorithms such as the MAP, particle filter (PF), and Kalman filter (KF). Simulation and real experiment results demonstrate that the proposed tracking algorithm provides an improvement roughly by 16%, 11%, and 18% over the MAP, PF, and KF, respectively, in the tracking accuracy.**

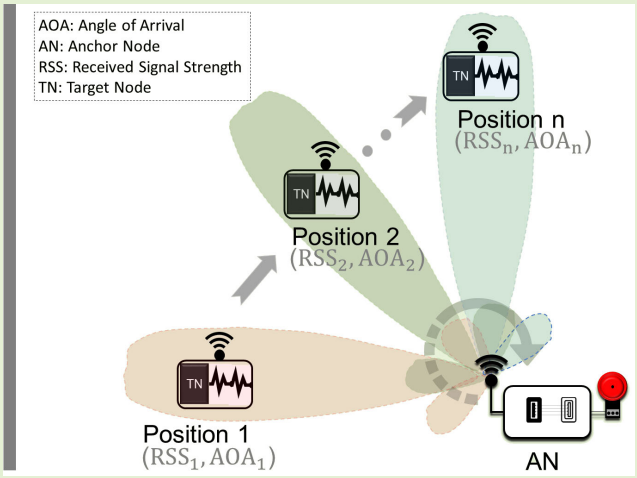

***Index Terms*— Angle of arrival (AOA), evolutionary algorithms, received signal strength (RSS), tracking, wireless sensor networks (WSNs).**

Manuscript received 3 May 2023; revised 12 August 2023; accepted 13 August 2023. Date of publication 30 August 2023; date of current version 2 October 2023. This work was supported in part by the National Research Foundation of Korea under Grant NRF-2021R1I1A1A01041257 and Grant NRF-2021M3A9E4080780 and in part by the Ministry of Trade, Industry, and Energy (MOTIE) under Grant RS-2023-00236325. The work of Iickho Song was supported by the Program of International Visiting Professor of the University of Science and Technology of China under Grant 2022BVT04. The associate editor coordinating the review of this article and approving it for publication was Prof. Mehmet Yuce. *(Corresponding authors: Lismer Andres Caceres Najarro; Youngtae Noh.)*

Lismer Andres Caceres Najarro, Muhammad Salman, and Youngtae Noh are with the School of Energy AI, Korea Institute of Energy and Technology, Naju 58330, Republic of Korea (e-mail: andrescn@kentech.ac.kr; salman@kentech.ac.kr; ytnoh@kentech.ac.kr).

Iickho Song is with the School of Electrical Engineering, Korea Advanced Institute of Science and Technology, Daejeon 34141, Republic of Korea, and also with the Department of Electronic Engineering and Information Science, University of Science and Technology of China, Hefei, Anhui 230026, China (e-mail: i.song@ieee.org).

Slavisa Tomic is with the Cognitive and People-Centric Computing Laboratory, Universidade Lusófona de Humanidades e Tecnologias, 1749-024 Lisbon, Portugal (e-mail: slavisa.tomic@ulusofona.pt).

Kiseon Kim is with the School of Electrical Engineering and Computer Science, Gwangju Institute of Science and Technology, Gwangju 61005, Republic of Korea (e-mail: kskim@gist.ac.kr).

Digital Object Identifier 10.1109/JSEN.2023.3308913

I. Introduction

TARGET nodes (TNs) in wireless sensor networks (WSNs) can be in a stationary or moving state. According to the state of the TNs, two types of localization problems can be categorized: stationary and moving localization problems. The latter is also known as the tracking problem. For localizing a stationary TN, several algorithms have been developed based on linear least squares, convex-relaxation, and machine learning [1]. Recently, evolution-based localization algorithms have been proven to be highly efficient and accurate [2], [3]. When localizing a moving TN (e.g., robots, submarines, and drones), algorithms based on Kalman filter (KF) and particle filter (PF) are the norm. The classical KF algorithm is known to be optimal in the sense of minimum mean square error for linear models with Gaussian noise distribution. Although variants of the KF such as the extended KF (EKF) and unscented KF (UKF) exist for nonlinear models, they have been shown to be unstable, i.e., they might not always converge [4].

Meanwhile, there exist several measurements that can be employed to track a TN such as the time of arrival, angle of arrival (AOA) [5], and received signal strength (RSS). Among these measurements, the RSS is very popular since

it is relatively straightforward to obtain without requiring sophisticated hardware. However, tracking algorithms based solely on RSS measurements commonly result in large tracking errors, especially when there are only a few anchor nodes (ANs) [6]. To mitigate such an undesirable result, in this article, we employ the RSS and AOA measurements simultaneously. There exist several works dealing with the tracking problem when only one type of measurement is used [6], [7], [8], [9], [10], [11], [12], [13], [14]. In contrast, there are only a few works dealing with the tracking problem when several types of measurements are employed simultaneously. In [15], the RSS and AOA were exploited for tracking a TN. Therein, the highly nonlinear observation model is first linearized and used with the KF for tracking a TN. Recently, a more sophisticated linearization technique, which uses conversion from Cartesian to polar coordinates, was employed for linearizing the observation model [4]. Then, by following the maximum a posteriori (MAP) criterion, a MAP algorithm was proposed and shown to provide better performance than the KF in [15]. It is shown in both [4] and [15] that the conventional PF outperformed the other techniques considered therein. More advanced PF techniques such as the one introduced in [7] may perform better. It is worth mentioning that, unlike the KF and MAP, the PF does not require approximations to deal with the nonlinearities of the tracking problem: this may be the reason why the PF usually outperforms the KF and MAP.

In this article, we propose and investigate an evolutionary algorithm that exploits the RSS and AOA measurements for tracking a moving TN. The tracking problem is formulated in the MAP framework which results in a highly nonlinear and nonconvex cost function of the tracking problem. Such a cost function cannot be directly handled by conventional techniques such as those based on KF and MAP which commonly leads to degradation of the tracking accuracy. We propose an evolutionary tracking algorithm based on the differential evolution (DE) that directly handles the highly nonlinear and nonconvex function without requiring any approximation, thus leading to an improvement in the tracking accuracy. The proposed algorithm exploits the opposition-based learning [16] and adaptive redirection [3] to enhance the search capability and redirection of individuals. A major concern in evolution-based algorithms is the proper tuning of control parameters on which the estimation accuracy is highly dependent. The tuning process is tedious and problem-specific in most of the cases. To relax such dependency, the proposed approach reformulates the mutation and crossover processes in such a way that the two control parameters, crossover probability, and mutation factor, do not need special care. Additionally, a population control procedure [17] is considered for possibly further improvement of the performance. Furthermore, the proposed approach takes into account the dynamic variation in the cost function of the tracking problem, resulting in better tracking accuracy. In summary, the main contributions of this article can be summarized as follows.

1) We propose and analyze a tracking algorithm based on the DE when the AOA and RSS measurements are employed simultaneously. The proposed algorithm does not require to relax the cost function of the tracking problem, which results in an improvement of the tracking accuracy.
2) The proposed algorithm reduces the dependence on control parameters, which can lead to an improvement in the tracking accuracy even in scenarios with constant variations of the environment.
3) To the best of our knowledge, this work is one of the very few, if not the first, to employ evolutionary algorithms for tracking purposes.
4) We validate the effectiveness of the proposed algorithm by using real data obtained in an indoor scenario.

The remainder of this article is organized as follows. In Section II, the RSS and AOA measurement models for the tracking problem of a moving TN are introduced. Section III presents the MAP framework and provides details of the proposed tracking algorithm. Simulation and real experiment results are presented in Section IV, where the proposed algorithm is compared with the KF, MAP, and PF algorithms in terms of the tracking accuracy and computational demand. Finally, Section V concludes this article.

II. Tracking Problem of TN

Assuming one TN, we deal with a 2-D WSN tracking problem as in [6], [7], [8], [9], [11], and [12]. Consider N ANs with fixed known positions $\boldsymbol{x}^{(n)} = [x^{(n)}, y^{(n)}]^{\mathrm{T}}$ for $n = 1, 2, \ldots, N$, and one moving TN with unknown position $\boldsymbol{x}_t = [x_t, y_t]^{\mathrm{T}}$ at time t, for $t = 1, 2, \ldots, T$.

Under the widely used path-loss model [3], [4], [18], the received power $P_t^{(n)}$ at the nth AN from the moving TN at time t can be expressed as

$$P_t^{(n)} = \rho^{(n)}(\boldsymbol{x}_t) + \mu_t^{(n)} \ (\mathrm{dB}) \tag{1}$$

where $\rho^{(n)}(\boldsymbol{x}_t) = P_0 - 10\gamma \log_{10}\|\boldsymbol{x}^{(n)} - \boldsymbol{x}_t\|$ is a function representing an ideal power decay with γ denoting the path loss exponent and P_0 being the power of the signal transmitted from the TN, for $n = 1, 2, \ldots, N$. Here, $\|\boldsymbol{\delta}\| = (\delta_1^2 + \delta_2^2)^{1/2}$ denotes the Euclidean norm of a vector $\boldsymbol{\delta} = [\delta_1, \delta_2]$ in the 2-D space $\mathbb{R}^2$. The additive noise term $\mu_t^{(n)}$ represents the log-shadowing effect, which follows a Gaussian distribution with mean zero and variance σ_μ^2, i.e., $\mu_t^{(n)} \sim \mathcal{N}(0, \sigma_\mu^2)$.

Meanwhile, the AOA measurement $\phi_t^{(n)}$ (in radian) between the nth AN and moving TN at time t can be modeled as

$$\phi_t^{(n)} = \alpha^{(n)}(\boldsymbol{x}_t) + m_t^{(n)} \tag{2}$$

where $\alpha^{(n)}(\boldsymbol{x}_t) = \arctan((y_t - y^{(n)})/(x_t - x^{(n)}))$ is a function capturing the angular relationship between the TN and AN at time t, and $m_t^{(n)} \sim \mathcal{N}(0, \sigma_m^2)$ represents the angular noise.

Taking (1) and (2) into consideration, the unknown position of the TN at time t can be estimated by solving the optimization problem

$$\hat{\boldsymbol{x}}_t = \arg\min_{\boldsymbol{x}_t} \tilde{f}(\boldsymbol{x}_t) \tag{3}$$

where

$$\tilde{f}(\boldsymbol{x}_t) = \sum_{n=1}^{N} \frac{1}{\sigma_\mu^2}\left(P_t^{(n)} - \rho^{(n)}(\boldsymbol{x}_t)\right)^2 + \sum_{n=1}^{N} \frac{1}{\sigma_m^2}\left(\phi_t^{(n)} - \alpha^{(n)}(\boldsymbol{x}_t)\right)^2 \quad (4)$$

represents the ML cost function when both the AOA and RSS measurements are employed simultaneously. Note that, for solving (3), several techniques developed for the stationary localization problem can be employed at each time t such as those based on linear least squares, semidefinite programming, and evolutionary algorithms [3]. However, such techniques disregard any prior knowledge that exists due to the movement of the TN.

In order to take into account existing prior knowledge of the TN, a constant velocity model is commonly employed [4], [7], which considers state and observation models. The state of a moving TN at time t can be defined by a state vector $\boldsymbol{\theta}_t = [\boldsymbol{x}_t^{\mathrm{T}}, \boldsymbol{v}_t^{\mathrm{T}}]^{\mathrm{T}}$, where $\boldsymbol{v}_t = [v_{t,x}, v_{t,y}]^{\mathrm{T}}$ denotes the speed of the TN at time t. The transition from state $\boldsymbol{\theta}_{t-1}$ to $\boldsymbol{\theta}_t$ is expressed by the state model as

$$\boldsymbol{\theta}_t = \boldsymbol{F}\boldsymbol{\theta}_{t-1} + \boldsymbol{e}_t \quad (5)$$

assuming a constant velocity, where

$$\boldsymbol{F} = \begin{bmatrix} 1 & 0 & T_s & 0 \\ 0 & 1 & 0 & T_s \\ 0 & 0 & 1 & 0 \\ 0 & 0 & 0 & 1 \end{bmatrix} \quad (6)$$

is the transition matrix and $\boldsymbol{e}_t \sim \mathcal{N}(\boldsymbol{0}, \boldsymbol{Q})$ denotes the state process noise with $\boldsymbol{Q}$ defined as

$$\boldsymbol{Q} = q\begin{bmatrix} \frac{T_s^3}{3} & 0 & \frac{T_s^2}{2} & 0 \\ 0 & \frac{T_s^3}{3} & 0 & \frac{T_s^2}{2} \\ \frac{T_s^2}{2} & 0 & T_s & 0 \\ 0 & \frac{T_s^2}{2} & 0 & T_s \end{bmatrix}. \quad (7)$$

Here, T_s and q denote the sampling period and intensity of the state noise process, respectively [19].

The observation model is expressed as

$$\boldsymbol{s}_t = \boldsymbol{h}(\boldsymbol{x}_t) + \boldsymbol{r}_t \quad (8)$$

where $\boldsymbol{s}_t \in \mathbb{R}^{2N}$ denotes the measurement vector, $\boldsymbol{h}(\boldsymbol{x}_t) = [\rho^{(1)}(\boldsymbol{x}_t), \rho^{(2)}(\boldsymbol{x}_t), \ldots, \rho^{(N)}(\boldsymbol{x}_t), \alpha^{(1)}(\boldsymbol{x}_t), \alpha^{(2)}(\boldsymbol{x}_t), \ldots, \alpha^{(N)}(\boldsymbol{x}_t)]^{\mathrm{T}}$, and $\boldsymbol{r}_t \sim \mathcal{N}(\boldsymbol{0}, \boldsymbol{R})$ represents the measurement noise vector with the covariance matrix $\boldsymbol{R} = \mathrm{diag}(\sigma_\mu^2, \sigma_\mu^2, \ldots, \sigma_\mu^2, \sigma_m^2, \sigma_m^2, \ldots, \sigma_m^2) \in \mathbb{R}^{2N\times 2N}$.

Then, the tracking problem consists of estimating the unknown state $\boldsymbol{\theta}_t$ of the moving TN from a history $\boldsymbol{s}_{1:t} = \{\boldsymbol{s}_1, \boldsymbol{s}_2, \ldots, \boldsymbol{s}_t\}$ of RSS and AOA measurements up to time t, given initial estimates $\hat{\boldsymbol{\theta}}_{0|0}$ and $\hat{\boldsymbol{C}}_{0|0}$ of the state vector and covariance matrix, respectively. Here, $\hat{\boldsymbol{\theta}}_{\tau_1|\tau_2}$ and $\hat{\boldsymbol{C}}_{\tau_1|\tau_2}$ denote the estimates of $\boldsymbol{\theta}_{\tau_1}$ and covariance matrix $\boldsymbol{C}_{\tau_1}$, respectively, at time τ_1 based on measurements $\boldsymbol{s}_{1:\tau_2}$, where $\boldsymbol{C}_t$ is the covariance matrix of the prior probability density function (pdf) of $\boldsymbol{\theta}_t$.

III. Proposed Tracking Algorithm

Since we have prior information about the position of the TN provided by the state model, we can formulate the tracking problem in the framework of MAP.

A. MAP Framework

The MAP framework allows us to estimate the state vector $\boldsymbol{\theta}_t$ by maximizing the posterior PDF $p(\boldsymbol{\theta}_t|\boldsymbol{s}_{1:t})$ as

$$\hat{\boldsymbol{\theta}}_{t|t} = \arg\max_{\boldsymbol{\theta}_t} p(\boldsymbol{\theta}_t|\boldsymbol{s}_{1:t}) \quad (9)$$

or, equivalently

$$\hat{\boldsymbol{\theta}}_{t|t} = \arg\max_{\boldsymbol{\theta}_t} (\ln p(\boldsymbol{s}_t|\boldsymbol{\theta}_t) + \ln p(\boldsymbol{\theta}_t|\boldsymbol{s}_{1:t-1})) \quad (10)$$

under the Markov condition on $\boldsymbol{s}_t$ [20], where $p(\boldsymbol{s}_t|\boldsymbol{\theta}_t)$ and $p(\boldsymbol{\theta}_t|\boldsymbol{s}_{1:t-1})$ denote the pdf of the measurement vector $\boldsymbol{s}_t$ parameterized by the state vector $\boldsymbol{\theta}_t$ and the prior pdf of $\boldsymbol{\theta}_t$ parameterized by the measurement vectors until time $t-1$, respectively.

From (8), the pdf $p(\boldsymbol{s}_t|\boldsymbol{\theta}_t)$ can be written as

$$p(\boldsymbol{s}_t|\boldsymbol{\theta}_t) = k_2 \exp\left(-\frac{1}{2}[\boldsymbol{s}_t - \boldsymbol{h}(\boldsymbol{x}_t)]^{\mathrm{T}}\boldsymbol{R}^{-1}[\boldsymbol{s}_t - \boldsymbol{h}(\boldsymbol{x}_t)]\right) \quad (11)$$

where k_2 is the normalizing constant. Since the prior pdf of $\boldsymbol{\theta}_t$ is difficult to obtain, it is commonly approximated by the Gaussian pdf as [15]

$$p(\boldsymbol{\theta}_t|\boldsymbol{s}_{1:t-1}) \approx k_1 \exp\left(-\frac{1}{2}\left[\boldsymbol{\theta}_t - \hat{\boldsymbol{\theta}}_{t|t-1}\right]^{\mathrm{T}}\hat{\boldsymbol{C}}_{t|t-1}^{-1}\left[\boldsymbol{\theta}_t - \hat{\boldsymbol{\theta}}_{t|t-1}\right]\right) \quad (12)$$

where k_1 is the normalizing constant. Here, from the state model (5) we get

$$\hat{\boldsymbol{\theta}}_{t|t-1} = \boldsymbol{F}\hat{\boldsymbol{\theta}}_{t-1|t-1} \quad (13)$$

and

$$\hat{\boldsymbol{C}}_{t|t-1} = \boldsymbol{F}\hat{\boldsymbol{C}}_{t-1|t-1}\boldsymbol{F}^{\mathrm{T}} + \boldsymbol{Q} \quad (14)$$

with the initial conditions $\hat{\boldsymbol{\theta}}_{0|0}$ and $\hat{\boldsymbol{C}}_{0|0}$.

By replacing (12) and (11) into (10), the MAP formulation for tracking the TN can be rewritten as

$$\hat{\boldsymbol{\theta}}_{t|t} = \arg\min_{\boldsymbol{\theta}_t} f(\boldsymbol{\theta}_t) \quad (15)$$

where

$$f(\boldsymbol{\theta}_t) = [\boldsymbol{s}_t - \boldsymbol{h}(\boldsymbol{x}_t)]^{\mathrm{T}}\boldsymbol{R}^{-1}[\boldsymbol{s}_t - \boldsymbol{h}(\boldsymbol{x}_t)] + \left[\boldsymbol{\theta}_t - \hat{\boldsymbol{\theta}}_{t|t-1}\right]^{\mathrm{T}}\hat{\boldsymbol{C}}_{t|t-1}^{-1}\left[\boldsymbol{\theta}_t - \hat{\boldsymbol{\theta}}_{t|t-1}\right] \quad (16)$$

is the MAP cost function.

B. Evolution-Based Tracking Algorithm

Instead of resorting to approximating the highly nonlinear and nonconvex cost function (16) of the MAP for the tracking problem, we introduce a novel tracking technique based on the DE. Although there exist evolutionary-based algorithms for localizing a TN [2], [3], [21], these algorithms cannot be directly applied to the tracking problem due to the dynamic

variations in the cost function of the MAP formulation. Additionally, the performance of such algorithms is affected by their control parameters. To mitigate aforementioned points, we propose an evolutionary tracking algorithm that adapts dynamically its control parameters to avoid possible degradation when locating the TN.

The proposed algorithm produces and exploits the population iteratively to find a global optimum. Here, the population at the gth generation is a set $\{\boldsymbol{I}_l^{(g)}\}_{l=1}^{L^{(g)}}$ of $L^{(g)}$ individuals, in which an individual $\boldsymbol{I}_l^{(g)} = [I_{l,1}^{(g)}, I_{l,2}^{(g)}, I_{l,3}^{(g)}, I_{l,4}^{(g)}]$ is a 4-D vector and is a candidate for an estimate $\hat{\boldsymbol{\theta}}_{t|t}$ of the unknown state vector $\boldsymbol{\theta}_t$.

The proposed algorithm is composed of seven processes, namely, generation of initial individuals, mutation, crossover, adaptive redirection, generation of opposite individuals, selection, and population reduction. It was pointed out that Gaussian sampling is a fine-tuning procedure that balances the exploitation and exploration paradigm in any evolutionary algorithm [22]. Based on that idea, the proposed approach employs Gaussian sampling in the generation of initial individuals, mutation, and crossover. Details of each of the processes are provided below.

1) Generation of Initial Individuals: Instead of generating randomly the initial population (at $g = 0$), we take advantage of the knowledge of the estimated state vector $\hat{\boldsymbol{\theta}}_{t-1}$ at time $t-1$ by sampling the Gaussian distribution as

$$\boldsymbol{I}_l^{(0)} \sim \mathcal{N}\left(\hat{\boldsymbol{\theta}}_{t|t-1}, \Delta_{t|t-1}\right) \tag{17}$$

for $l = 1, 2, \ldots, L^{(0)}$, where $L^{(0)}$ denotes the size of initial population and $\Delta_{t|t-1} = \text{diag}(\sigma_1^2, \sigma_2^2, \sigma_3^2, \sigma_4^2)$ with $\{\sigma_i^2\}_{i=1}^4$ being the diagonal elements of $\hat{\boldsymbol{C}}_{t|t-1}$.

2) Mutation: The population $\{\boldsymbol{I}_l^{(g)}\}_{l=1}^{L^{(g)}}$ is employed for creating a mutant population

$$\tilde{\boldsymbol{I}}_l^{(g)} \sim \mathcal{N}\left(\frac{\boldsymbol{I}^{(g)} + \boldsymbol{I}_l^{(g)}}{2}, \boldsymbol{\Upsilon}^{(g)}\right) \tag{18}$$

by sampling the Gaussian distribution, where

$$\boldsymbol{I}^{(g)} = \arg\min_{\boldsymbol{I}_l^{(g)}} \left\{ f\left(\boldsymbol{I}_l^{(g)}\right) \right\}_{l=1}^{L^{(g)}} \tag{19}$$

is the best individual at the gth generation and $\boldsymbol{\Upsilon}^{(g)} = \text{diag}(|I_1^{(g)} - I_{l,1}^{(g)}|^2, |I_2^{(g)} - I_{l,2}^{(g)}|^2, |I_3^{(g)} - I_{l,3}^{(g)}|^2, |I_4^{(g)} - I_{l,4}^{(g)}|^2)$.

3) Crossover: The trial population $\{\check{\boldsymbol{I}}_l^{(g)}\}_{l=1}^{L^{(g)}}$ is obtained as

$$\check{I}_{l,d}^{(g)} = \begin{cases} \tilde{I}_{l,d}^{(g)}, & \text{if } c_l \le p_{C_l}^{(g)} \text{ or } d = d_r \\ I_{l,d}^{(g)}, & \text{otherwise} \end{cases} \tag{20}$$

by employing a standard crossover, where $d_r \in \{1, 2, 3, 4\}$ is a random index and $c_l \sim \mathcal{U}(0, 1)$, the uniform distribution on $(0, 1)$.

In many cases, the crossover probability $p_{C_l}^{(g)}$ is fixed based on a laborious error and trial process [3]. In contrast, in this work, the parameter $p_{C_l}^{(g)}$ is generated by dynamically sampling a Gaussian distribution as

$$p_{C_l}^{(g)} \sim \mathcal{N}\left(\exp\left(\acute{f}_l^{(g)} - \bar{f}_l^{(g)}\right), 0.1^2\right) \tag{21}$$

where $\acute{f}_l^{(g)}$ and $\bar{f}_l^{(g)}$ represent the minimum and average values of the MAP cost function (16) over the $L^{(g)}$ individuals at the gth generation. The parameter $p_{C_l}^{(g)}$ plays a crucial role in influencing the exploration and exploitation capabilities of the algorithm. Lower values of $p_{C_l}^{(g)}$ promote exploitation, leading to a faster convergence, while higher values of $p_{C_l}^{(g)}$ promote exploration which helps to prevent premature convergence to local optimum. Therefore, it is important to carefully control the values of this parameter. A way to do that is to increase or decrease the value of $p_{C_l}^{(g)}$ proportionally to the convergence of the algorithm [23]. To detect the convergence of the algorithm, we can check the difference between $\acute{f}_l^{(g)}$ and $\bar{f}_l^{(g)}$ [24]. Note that we have chosen the exponential function in (21) because it translates a possible local convergence into a high value of $p_{C_l}^{(g)}$ at a higher rate than, for example, a linear function. The standard deviation in (21) is set up to small value of 0.1 to guarantee that most of the values of $p_{C_l}^{(g)}$ generated by (21) are in the recommended interval [0, 1] [25] even when $p_{C_l}^{(g)}$ is near 0 or 1.

4) Adaptive Redirection: This procedure guides the individuals inside solution space is defined as

$$\mathbf{Z} = \{(z_1, z_2, z_3, z_4) : a_i \le z_i \le b_i, i \in \{1, 2, 3, 4\}\} \tag{22}$$

where $\boldsymbol{a} = [a_1, a_2, a_3, a_4]$ and $\boldsymbol{b} = [b_1, b_2, b_3, b_4]$ denote the vectors of lower and upper bounds, respectively. Specifically, the redirected population $\{\dot{\boldsymbol{I}}_l^{(g)}\}_{l=1}^{L^{(g)}}$ is obtained as

$$\dot{I}_{l,d}^{(g)} = \begin{cases} \check{I}_{l,d}^{(g)}, & \text{if } a_d \le \check{I}_{l,d}^{(g)} \le b_d \\ \beta_d\left(b_d^{(g)} - a_d^{(g)}\right) + a_d^{(g)}, & \\ & \text{if } \check{I}_{l,d}^{(g)} < a_d \text{ or } \check{I}_{l,d}^{(g)} > b_d \end{cases} \tag{23}$$

from the trial population $\{\check{\boldsymbol{I}}_l^{(g)}\}_{l=1}^{L^{(g)}}$, where $\beta_d \sim \mathcal{U}(0, 1)$, and

$$a_d^{(g)} = \min_{I_{l,d}^{(g)}}\left(\left\{I_{l,d}^{(g)}\right\}_{l=1}^{L^{(g)}}\right) \tag{24}$$

and

$$b_d^{(g)} = \max_{I_{l,d}^{(g)}}\left(\left\{I_{l,d}^{(g)}\right\}_{l=1}^{L^{(g)}}\right) \tag{25}$$

represent the lower and upper bounds, respectively, of the area of redirection at the gth generation.

5) Generation of Opposite Individuals: The opposite individual is generated from the redirected individual as [26]

$$\ddot{\boldsymbol{I}}_l^{(g)} = \boldsymbol{a}^{(g)} + \boldsymbol{b}^{(g)} - \dot{\boldsymbol{I}}_l^{(g)} \tag{26}$$

where $\boldsymbol{a}^{(g)} = [a_1^{(g)}, a_2^{(g)}, a_3^{(g)}, a_4^{(g)}]$ and $\boldsymbol{b}^{(g)} = [b_1^{(g)}, b_2^{(g)}, b_3^{(g)}, b_4^{(g)}]$.

6) Selection: An individual with the lowest fitness value among the original, redirected, and opposite to the redirected individuals is selected as

$$\boldsymbol{I}_l^{(g+1)} = \arg\min_{\boldsymbol{I}_l^{(g)}, \dot{\boldsymbol{I}}_l^{(g)}, \ddot{\boldsymbol{I}}_l^{(g)}} \left\{ f\left(\boldsymbol{I}_l^{(g)}\right), f\left(\dot{\boldsymbol{I}}_l^{(g)}\right), f\left(\ddot{\boldsymbol{I}}_l^{(g)}\right) \right\} \tag{27}$$

for $l = 1, 2, \ldots, L^{(g)}$, which is then used as the initial individual in the next generation.

Algorithm 1 Evolutionary Tracking Algorithm

Input: MAP cost function (16), RSS and AOA measurements, number N of ANs, size $L^{(0)}$ of initial population, covariance $\boldsymbol{Q}$ of the state process noise, transition matrix $\boldsymbol{F}$, covariance $\boldsymbol{R}$ of the observation model, maximum number G of generations, lower bounds a_d, and upper bounds b_d for $d = 1, 2, 3, 4$

Output: Estimated value of the state vector $\hat{\boldsymbol{\theta}}_t$

Initialization: $\hat{\boldsymbol{\theta}}_{0|0}$ by solving (3), $\hat{\boldsymbol{C}}_{0|0} = \mathbf{I}_4$
for $t = 1, 2, \ldots, T-1$ **do**
  Prediction: Obtain $\hat{\boldsymbol{\theta}}_{t|t-1}$ and $\hat{\boldsymbol{C}}_{t|t-1}$ by solving (13) and (14), respectively.
  Update: Obtain $\hat{\boldsymbol{\theta}}_{t|t}$ by:;
  → Initialize the population according to (17);
  while $g \leq G-1$ **do**
    for $l = 1; l \leq L; l = l+1$ **do**
      → Create mutant individuals with (18);
      → Generate trial individuals via (20);
      → Redirect the individuals via (23);
      → Create opposite individuals with (26);
      → Select the best individual via (27);
    end
    → Adapt the population according to (28);
    Increase $g = g+1$;
  end
  Return the estimated value of the state vector $\boldsymbol{\theta}_t$;
end

7) Population Control: It was shown that by reducing the population size in a variant of the DE, an improvement of the accuracy can be obtained [27]. Additionally, a reduction in the size of the population relaxes the computational burden. Inspired by these findings, here we implement a population size reduction technique that carefully reduces the population size generation by generation following a parabolic decay as [17]

$$L^{(g+1)} = \left\lceil \frac{L^{(0)} - \underrightarrow{L}}{G^2}(g-G)^2 + \underrightarrow{L} \right\rceil \tag{28}$$

where $\underrightarrow{L}$ denotes the pre-defined minimum number of individuals required in the evolution process. When reducing the size of the population, the least favorable individuals are eliminated.

After G generations, the best individual

$$\boldsymbol{I}' = \arg\min_{\boldsymbol{I}_l^{(G)}} \left\{ f\left(\boldsymbol{I}_l^{(G)}\right) \right\}_{l=1}^{L^{(G)}} \tag{29}$$

among $\{\boldsymbol{I}_l^{(G)}\}_{l=1}^{L^{(G)}}$ is selected and presented as the estimate $\hat{\boldsymbol{\theta}}_t$ of the vector state $\boldsymbol{\theta}_t$. The pseudocode of the proposed tracking algorithm is summarized in Algorithm 1.

IV. Tracking Performance

In this section, we assess the tracking performance of the proposed algorithm. For comparison, we consider three recently developed algorithms, the KF [4], MAP [4], and PF [7]. The tracking accuracy of the algorithms at each time t is evaluated and compared based on the root-mean-square error (RMSE) defined as

$$\text{RMSE}_t = \sqrt{\frac{1}{K}\sum_{k=1}^{K} \left\| \hat{\boldsymbol{x}}_{t,k} - \boldsymbol{x}_{t,k} \right\|^2} \tag{30}$$

where K is the number of Monte Carlo trials and $\boldsymbol{x}_{t,k}$ and $\hat{\boldsymbol{x}}_{t,k}$ denote the actual and estimated positions, respectively, of the TN at time t in the kth Monte Carlo trial.

For a complete trajectory of the TN, 1000 Monte Carlo trials are considered. The measurement vector $\boldsymbol{s}_t$ is generated with the following considerations: $P_0 = -10$ dBm for the transmit power of the TN, $\gamma = 3$ for the path loss exponent, and $\sigma_\mu = 9$ dB and $\sigma_m = 4$ degrees, respectively, for the standard deviation of the log-shadowing and angular noise. Additionally, the noise intensity for the state process is set to $q = 2.5 \times 10^{-3}$ m^2/s^3. The RSS and AOA measurements are sampled at every $T_s = 1$ s. For the control parameters of the proposed algorithm, we assume the size $L^{(0)} = 20$ of the initial population and a maximum number $G = 50$ of generations as in [28]. For the control parameter of the PF, we consider 1000 particles as in [7].

A. Effects of Different Trajectories

We have considered three tracking scenarios in which the TN maintains a straight route performs sharp maneuvers, and executes moderate maneuvers. These scenarios are represented by deterministic trajectories of a straight line, rectangle, and circle as shown in Fig. 1(a)–(c), respectively. An area of interest of 40×40 m with four ANs deployed at fixed locations $(0, 0)$, $(40, 40)$, $(0, 40)$, and $(40, 0)$ is considered. The TN starts to move counterclockwise at the positions $(5, 5)$, $(7, 10)$, and $(10, 20)$, over $T = 30$ s, $T = 80$ s, and $T = 40$ s with a speed of 1 m/s for the trajectories illustrated in Fig. 1(a)–(c), respectively. The position of the TN is bounded by the area of interest with the lower and upper bounds being $a_1 = a_2 = 0$ and $b_1 = b_2 = 40$, respectively. The lower and upper bounds for the unknown velocity are set to $a_3 = a_4 = 0$ and $b_3 = b_4 = 2$, respectively.

Fig. 1 depicts the true and estimated trajectories of the proposed, KF, MAP, and PF for the three scenarios considered here. Although not completely clear, it is observed that the estimated trajectory of the proposed algorithm is closer to the ground-truth than those of the other algorithms, especially when the TN follows the straight trajectory depicted in Fig. 1(a). Additionally, it is observed that there is a deterioration of the performance of all the algorithms when there exist variations in the trajectory of the TN, especially sharp ones. This outcome is not surprising as the abrupt change of the direction of the TN would impair the prior knowledge of the TN exploited by the algorithms.

Fig. 2 shows the RMSE of the algorithms as a function of the time for the three trajectories depicted in Fig. 1. It is clearly observed that the proposed algorithm outperforms the other algorithms over almost the whole trajectories of the TN. This figure also shows that all the algorithms are more stable

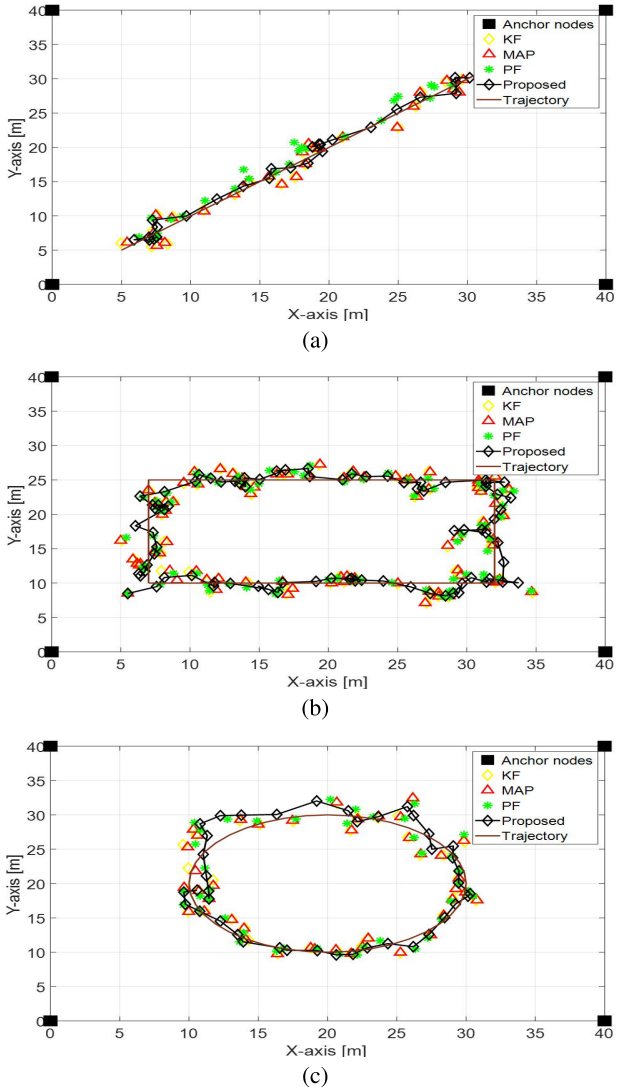

Fig. 1. One trial estimated trajectories of the algorithms when the TN follows (a) linear, (b) rectangle, and (c) circle trajectories (ground-truth).

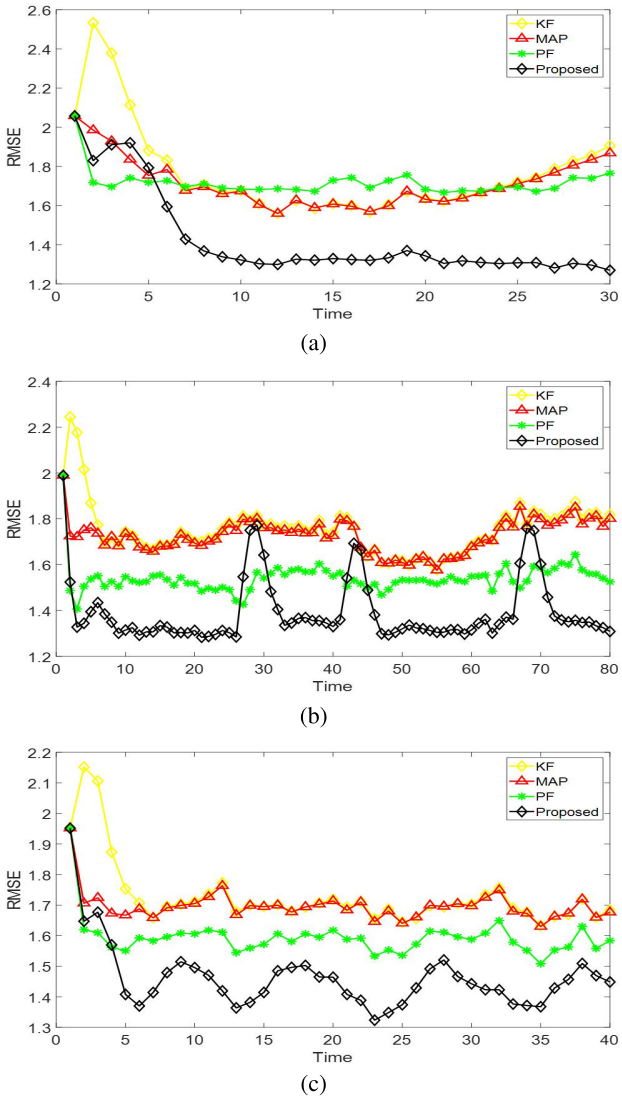

Fig. 2. RMSE of several algorithms at each time for the trajectories depicted in (a) Fig. 1(a), (b) Fig. 1(b), and (c) Fig. 1(c).

when there is no or few changes in the direction of the TN. The proposed algorithm is clearly the most stable one among the algorithms when there is no changes in the direction of the TN as in Fig. 1(a). In the meantime, the stability of the proposed algorithm seems to be affected more than the other algorithms by changes, especially sharp ones, in the direction of the TN as shown in Fig. 2(b) and (c). This result implies that the accuracy of the proposed algorithm is dependent more on the prior knowledge of the TN than that of other algorithms is.

The average RMSE over each of the trajectories is shown in Table I. Based on these results, we can state that the proposed approach improves the tracking accuracy by approximately 9%–20%, 8%–15%, and 15%–18% with respect to the other approaches in the scenarios considered in Fig. 1(a)–(c), respectively. Additionally, Table II illustrates the mean and standard deviation of the RMSE at positions [10, 10], [20, 20], and [30, 30]. This table shows that the proposed algorithm provides the smallest mean and standard deviation values of the RMSE

TABLE I
AVERAGE RMSE OF ALGORITHMS OVER THE COMPLETE TRAJECTORIES CONSIDERED IN FIG. 1

Algorithm:	KF	MAP	PF	Proposed
Linear:	1.78	1.72	1.72	1.44
Rectangle:	1.76	1.73	1.54	1.40
Circle:	1.73	1.70	1.59	1.46

at the three positions of the TN. These results demonstrate that the proposed algorithm is the most accurate and stable at the considered positions.

B. Effect of Control Parameters

In contrast to the standard DE, the proposed algorithm has mainly two control parameters: the size $L^{(0)}$ of the initial population and the maximum number G of iterations. To see the effect of these two control parameters on the tracking accuracy, we vary their values from 5 to 100 and calculate the average RMSE for a complete trajectory at each of the

TABLE II
MEAN AND STANDARD DEVIATION OF THE RMSE AT THREE POSITIONS OF THE TN

	Position 1: $[10, 10]$ mean / std (m)	**Position 2**: $[20, 20]$ mean / std (m)	**Position 3**: $[30, 30]$ mean / std (m)
KF	3.32/3.46	2.58/2.63	3.11/3.05
MAP	3.17/3.28	2.57/2.63	3.08/2.99
PF	2.98/2.89	2.93/2.82	2.85/2.94
Proposed	2.48/2.78	1.79/1.83	1.66/1.74

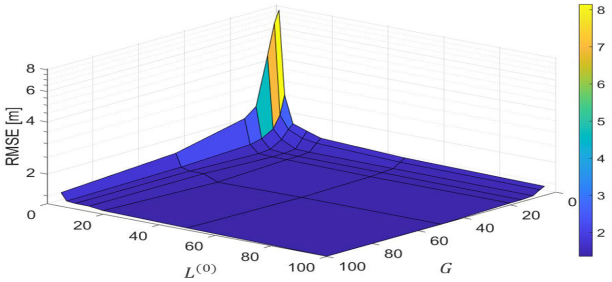

Fig. 3. Average RMSE versus the size $L^{(0)}$ of initial population and maximum number G of iteration for the linear trajectory.

TABLE III
AVERAGE RMSE OVER THE COMPLETE TRAJECTORY CONSIDERED IN FIG. 1(a) WITH AND WITHOUT INACCURATE PRIOR KNOWLEDGE

Algorithm:	KF	MAP	PF	Proposed
With:	1.82	1.75	1.81	1.64
Without:	1.78	1.72	1.72	1.44

values of $L^{(0)}$ and G. Under the same scenario of the tracking problem with the same distribution of ANs and trajectory of a TN as in Figs. 1(a) and 3 shows the average RMSE versus $L^{(0)}$ and G. It is observed that the proposed algorithm provides better tracking accuracy as $L^{(0)}$ and G increase until $L^{(0)} \approx 20$ and $G \approx 50$ approximately. It is also observed that the proposed algorithm does not exhibit significant improvement of the tracking accuracy for $L^{(0)} > 20$ and $G > 50$.

C. Effect of Inaccurate Prior Knowledge

To evaluate the impact of inaccurate prior knowledge, we introduced Gaussian noise with zero mean and a standard deviation of 0.5 to the estimated positions of the TN for all compared algorithms throughout the complete trajectory. Table III shows the average RMSE for the algorithms with and without inaccurate prior knowledge. Notably, all algorithms show a decrease in tracking accuracy when inaccurate prior knowledge is introduced. Although the proposed PF algorithms are the most affected, the proposed algorithm still provides the best tracking accuracy.

D. Computational Complexity

To describe the complexity of the algorithms, let us adopt the *Big-O* notation. By neglecting minor terms, the complexity of the algorithms is represented only by the dominant terms, i.e., the maximum number G of iteration, size $L^{(g)}$ of population at the gth generation, number N of ANs, number P of particles, and dimension $\mathcal{J}$ of the state vector. Table IV shows the theoretical complexity of the algorithms compared. It is observed that the theoretical complexity of the proposed algorithm, KF, MAP, and PF is of the order of N^3, N^3, N^2, and N^3, respectively. Similarly, the proposed algorithm, KF, MAP, and PF is of the order of $\mathcal{J}^3$, $\mathcal{J}$, $\mathcal{J}^2$, and $\mathcal{J}^2$, respectively.

TABLE IV
THEORETICAL COMPUTATIONAL COMPLEXITY

Algorithm	**Complexity**
KF	$O(\mathcal{J}N^2 + N^3)$
MAP	$O(\mathcal{J}^2N + \mathcal{J}^3)$
PF	$O(P(\mathcal{J}^2N + N^2))$
Proposed	$O(GL^{(g)}(\mathcal{J}^3 + N^3))$

TABLE V
AVERAGE RUNNING TIME (CPU: INTEL CORE[2] I5-6600 3.30 GHz. RAM: 16.0 GB)

Algorithm:	KF	MAP	PF	Proposed
Time (ms):	0.07	0.16	21.75	100.30

Assuming the same values of parameters as those shown in Fig. 2, measurements from real computation time were secured. The average running time in millisecond is presented in Table V. The table reveals that the proposed algorithm requires the longest running time, while the KF algorithm requires the shortest running time. Despite having the highest computational demand among the compared algorithms, the proposed scheme is still acceptable for real-time applications. Hence, the proposed algorithm offers a good trade-off between accuracy and computational requirement. It is worth mentioning that by adjusting the maximum number G of generations and the size $L^{(0)}$ of initial population [which is intrinsically linked with the size $L^{(g)}$ of population at the gth generation through (28)] the tracking accuracy and the running time of the proposed algorithm can be controlled to a certain extent. Increased G and $L^{(0)}$ implies improved tracking accuracy at the cost of longer running time. Conversely, reducing G and/or $L^{(0)}$ will result in lower tracking accuracy and reduced running time. These observations are supported by the results presented in Fig. 3 and Table IV.

E. Real Tracking Experiment

To verify and validate the performance of the proposed tracking algorithm, we employ measurements obtained in [29] for indoor scenarios under real conditions where nonline-of-sight, multipath propagation, and severe signal attenuation exist.

Each AN was equipped with a high-performance 2 Mb/s Lucent-802.11 card, which was connected to a Hyperlink

[1]Registered trademark.
[2]Trademarked.

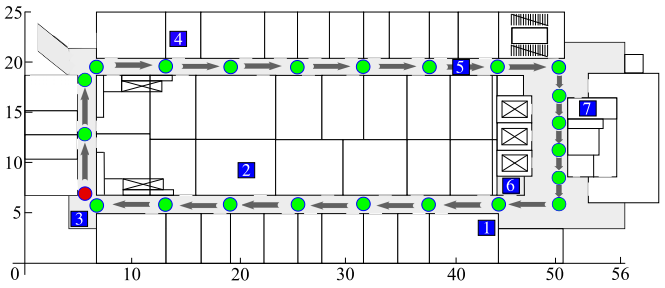

Fig. 4. Tracking setup in real indoor environment: Seven ANs (blue squares) and a TN moving clockwise.

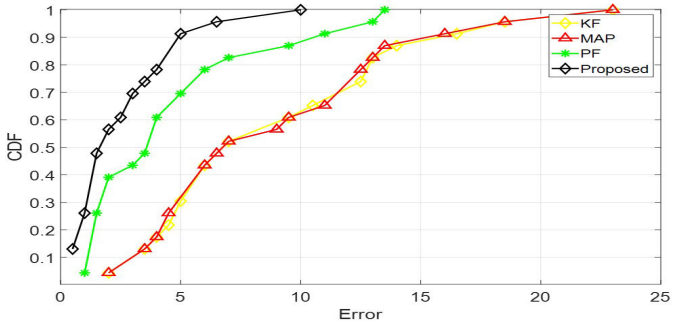

Fig. 5. CDF of tracking error of several algorithms under real measurements.

directional antenna with a gain of 14 dB. The TN is a standard laptop equipped with an 802.11 Wi-Fi card. The antennas of the ANs and TN were set up to provide a horizontal radiation pattern. At each AN, measurements of RSS and AOA from the TN were obtained. To ensure comprehensive data representation, the RSS and AOA measurements were taken at various times throughout the day and night, including peak hours during busy mornings and afternoons.

Fig. 4 shows the layout of the 56 × 25 m scenario where the RSS and AOA measurements took place. The seven blue squares and 23 circles represent the position of the ANs and the positions (ground-truth) where the RSS and AOA measurements were obtained from the TN. The red circle represents the initial position of the TN, which moves clockwise.

Fig. 5 shows the cumulative distribution function (cdf) of the tracking error $\|\hat{\boldsymbol{x}}_t - \boldsymbol{x}_t\|$. It is clearly observed that the proposed algorithm outperforms the other algorithms. Additionally, the proposed algorithm achieves a tracking error $\leq$5 m in 90% of the cases while the value for the KF, MAP, and PF is lower than 30%, 30%, and 70%, respectively.

F. Limitations

In Sections IV-A, IV-C, and IV-E, simulations and real experiments demonstrate that the proposed algorithm provides higher tracking accuracy. However, we would like to acknowledge that there exist certain factors that may impose limitations on its performance. For instance, although the proposed algorithm has fewer control parameters, i.e., only G and $L^{(0)}$, than standard evolutionary algorithms, such parameters affect not only the tracking accuracy but also the computational complexity (See Table IV). Therefore, finding appropriate values for these control parameters requires extra effort. Additionally, we have shown in Section IV-D that the proposed algorithm is computationally demanding. Consequently, if we increase the simulation period, the total required time for the complete simulation may increase accordingly. Moreover, as in the other algorithms, an increase in the area of interest may lead to a degradation of tracking accuracy, particularly in indoor environments, as the RSS and AOA measurements deteriorate.

V. Conclusion

We have addressed the tracking problem of a TN based on combined RSS and AOA measurements. The tracking problem has been formulated in the framework of the MAP, in which the prior knowledge of a moving TN is exploited. We have proposed a tracking approach based on an evolution algorithm, which takes advantage of the opposition-based learning and adaptive redirection. The proposed approach takes into account the prior knowledge of the position of a moving TN to enhance the tracking accuracy. The proposed algorithm was compared with the KF, MAP, and PF algorithms in three particular trajectories: linear, rectangular, and circular. Simulation results showed that the proposed algorithm outperformed the other algorithms over most portion of the trajectories, reducing the tracking error by more than 8% on average. A real indoor tracking experiment validates additionally the effectiveness of the proposed algorithm.

Acknowledgment

The authors would like to thank the Associate Editor and two anonymous reviewers for their constructive suggestions and helpful comments.

References

[1] L. A. Caceres Najarro, I. Song, and K. Kim, "Fundamental limitations and state-of-the-art solutions for target node localization in WSNs: A review," *IEEE Sensors J.*, vol. 22, no. 24, pp. 23661–23682, Dec. 2022.

[2] S. D. Correia, M. Beko, S. Tomic, and L. A. D. S. Cruz, "Energy-based acoustic localization by improved elephant herding optimization," *IEEE Access*, vol. 8, pp. 28548–28559, 2020.

[3] L. A. Caceres Najarro, I. Song, and K. Kim, "Differential evolution with opposition and redirection for source localization using RSS measurements in wireless sensor networks," *IEEE Trans. Autom. Sci. Eng.*, vol. 17, no. 4, pp. 1736–1747, Oct. 2020.

[4] S. Tomic, M. Beko, R. Dinis, M. Tuba, and N. Bacanin, "Bayesian methodology for target tracking using combined RSS and AoA measurements," *Phys. Commun.*, vol. 25, pp. 158–166, Dec. 2017.

[5] L. Calkins, P. Baldoni, J. McMahon, C. Wilhelmi, and M. M. Zavlanos, "Bearing-only active sensing under merged measurements," *IEEE Robot. Autom. Lett.*, vol. 6, no. 3, pp. 4544–4551, Jul. 2021.

[6] K. Wen, C. K. Seow, and S. Y. Tan, "An indoor localization and tracking system using successive weighted RSS projection," *IEEE Antennas Wireless Propag. Lett.*, vol. 19, no. 9, pp. 1620–1624, Sep. 2020.

[7] Z. Li and T. Braun, "Passively track WiFi users with an enhanced particle filter using power-based ranging," *IEEE Trans. Wireless Commun.*, vol. 16, no. 11, pp. 7305–7318, Nov. 2017.

[8] N. H. Nguyen and K. Doğançay, "Instrumental variable based Kalman filter algorithm for three-dimensional AoA target tracking," *IEEE Signal Process. Lett.*, vol. 25, no. 10, pp. 1605–1609, Oct. 2018.

[9] Y.-M. Pun and A. M. So, "Local strong convexity of source localization and error bound for target tracking under time-of-arrival measurements," *IEEE Trans. Signal Process.*, vol. 70, pp. 190–201, 2022.

[10] X. Fang and L. Chen, "An optimal multi-channel trilateration localization algorithm by radio-multipath multi-objective evolution in RSS-ranging-based wireless sensor networks," *Sensors*, vol. 20, no. 6, p. 1798, Mar. 2020.

[11] D. Biswas, S. Barai, and B. Sau, "Enhanced RSSI-based real-time position-tracking system in vehicular networks," *IEEE Sensors Lett.*, vol. 6, no. 6, pp. 1–4, Jun. 2022.

[12] S. R. Jondhale, R. Maheswar, and J. Lloret, *Received Signal Strength Based Target Localization and Tracking Using Wireless Sensor Networks* (EAI/Springer Innovations in Communication and Computing (EAIS-ICC)). Berlin, Germany: Springer, 2022.

[13] S. R. Jondhale, A. S. Jondhale, P. S. Deshpande, and J. Lloret, "Improved trilateration for indoor localization: Neural network and centroid-based approach," *Int. J. Distrib. Sensor Netw.*, vol. 17, no. 11, pp. 1–14, Nov. 2021.

[14] S. R. Jondhale, M. A. Wakchaure, B. S. Agarkar, and S. B. Tambe, "Improved generalized regression neural network for target localization," *Wireless Pers. Commun.*, vol. 125, no. 2, pp. 1677–1693, Mar. 2022.

[15] M. W. Khan, A. H. Kemp, N. Salman, and L. S. Mihaylova, "Tracking of wireless mobile nodes in he presence of unknown path-loss characteristics," in *Proc. Int. Conf. Informat. Fusion*, Washington, DC, USA, Jul. 2015, pp. 104–111.

[16] Z. Seif and M. B. Ahmadi, "An opposition-based algorithm for function optimization," *Eng. Appl. Artif. Intell.*, vol. 37, pp. 293–306, Jan. 2015.

[17] L. A. Caceres Najarro, I. Song, and K. Kim, "Adaptation of population size in differential evolution and its effects on localization of target nodes," *IEEE Access*, vol. 10, pp. 107785–107798, 2022.

[18] Y. Zou and H. Liu, "RSS-based target localization with unknown model parameters and sensor position errors," *IEEE Trans. Veh. Technol.*, vol. 70, no. 7, pp. 6969–6982, Jul. 2021.

[19] N. H. Nguyen and K. Dogançay, "Improved pseudolinear Kalman filter algorithms for bearings-only target tracking," *IEEE Trans. Signal Process.*, vol. 65, no. 23, pp. 6119–6134, Dec. 2017.

[20] K. P. Murphy, "Dynamic Bayesian networks: Representation, inference and learning," Ph.D. thesis, Dept. Comput. Sci., University of California, Berkeley, Berkeley, CA, UA, 2002.

[21] Z. Lalama, S. Boulfekhar, and F. Semechedine, "Localization optimization in WSNs using meta-heuristics optimization algorithms: A survey," *Wireless Pers. Commun.*, vol. 122, no. 2, pp. 1197–1220, Jan. 2022.

[22] Z. He, H. Peng, C. Deng, Y. Tan, Z. Wu, and S. Wu, "A spark-based Gaussian bare-bones cuckoo search with dynamic parameter selection," in *Proc. IEEE Congr. Evol. Comput.*, Wellington, New Zealand, Jun. 2019, pp. 1220–1227.

[23] R. D. Al-Dabbagh, F. Neri, N. Idris, and M. S. Baba, "Algorithmic design issues in adaptive differential evolution schemes: Review and taxonomy," *Swarm Evol. Comput.*, vol. 43, pp. 284–311, Dec. 2018.

[24] M. Srinivas and L. M. Patnaik, "Adaptive probabilities of crossover and mutation in genetic algorithms," *IEEE Trans. Syst., Man, Cybern.*, vol. 24, no. 4, pp. 656–667, Apr. 1994.

[25] R. Storn and K. Price, "Differential evolution—A simple and efficient heuristic for global optimization over continuous spaces," *IEEE J. Global Optim.*, vol. 11, no. 4, pp. 341–359, Dec. 1997.

[26] H. R. Tizhoosh, "Opposition-based learning: A new scheme for machine intelligence," in *Proc. Int. Conf. Comput.*, Vienna, Austria, Nov. 2005, pp. 695–701.

[27] R. Tanabe and A. S. Fukunaga, "Improving the search performance of SHADE using linear population size reduction," in *Proc. IEEE Congr. Evol. Comput. (CEC)*, Jul. 2014, pp. 1658–1665.

[28] L. A. Caceres Najarro, I. Song, S. Tomic, and K. Kim, "Fast localization with unknown transmit power and path-loss exponent in WSNs based on RSS measurements," *IEEE Commun. Lett.*, vol. 24, no. 12, pp. 2756–2760, Dec. 2020.

[29] D. Niculescu and B. Nath, "VOR base stations for indoor 802.11 positioning," in *Proc. 10th Annu. Int. Conf. Mobile Comput. Netw.*, Philadelphia, PA, USA, Sep. 2004, pp. 58–69.

Lismer Andres Caceres Najarro received the B.Sc. degree from the Peruvian University of Applied Sciences, Lima, Peru, in 2010, the M.S. degree from Kyungsung University, Busan, Republic of Korea, in 2016, and the Ph.D. degree in electrical engineering and computer science from the Gwangju Institute of Science and Technology (GIST), Gwangju, Republic of Korea, in 2021.

He is currently a Research Professor with the Energy AI, Korean Institute of Energy and Technology (KENTECH), Naju, Republic of Korea. Before joining KENTECH he worked as a Principal Investigator at the Information Communication Convergence Research Center-GIST from 2021 to 2023. His research interests include target localization in wireless sensor networks, evolutionary algorithms, machine learning, multi-agent systems, smart grids, and smart healthcare.

Dr. Caceres Najarro was awarded the Graña y Montero Peruvian Engineering Research Award, fourth edition.

Iickho Song (Fellow, IEEE) received the B.S.E. (magna cum laude) and M.S.E. degrees in electronics engineering from Seoul National University, Seoul, South Korea, in 1982 and 1984, respectively, and the M.S.E. and Ph.D. degrees in electrical engineering from the University of Pennsylvania, Philadelphia, PA, USA, in 1985 and 1987, respectively.

He was a member of the Technical Staff at Bell Communications Research, Morristown, NJ, USA, in 1987. In 1988, he joined the School of Electrical Engineering, Korea Advanced Institute of Science and Technology, Seoul, where he is currently a Professor. He has coauthored few books including *Advanced Theory of Signal Detection* (Springer, 2002), *Random Variables and Stochastic Processes* (Korean, Freedom Academy, 2014), and *Probability and Random Variables: Theory and Applications* (Springer, 2022); and has published papers on signal detection and mobile communications.

Prof. Song is a Fellow of the Korean Academy of Science and Technology (KAST), the IET, and the Korean Institute of Communications and Information Sciences (KICS), and a member of the Acoustical Society of Korea (ASK), the Institute of Electronics Engineers of Korea (IEEK), and the Korea Institute of Information, Electronics, and Communication Technology. He has received several awards including the Young Scientists Award (KAST) in 2000, the Achievement Award (IET) in 2006, and the Hae Dong Information and Communications Academic Award (KICS) in 2006. He has served as the Treasurer for the IEEE Korea Section, an Editor for the *Journal of the ASK*, *Journal of the IEEK*, *Journal of the KICS*, *Journal of Communications and Networks* (JCN), and a Division Editor for the *Journal of Communications and Networks* (JCN).

Slavisa Tomic received the M.S. degree in traffic engineering according to the postal traffic and telecommunications study program from the University of Novi Sad, Novi Sad, Serbia, in 2010, and the Ph.D. degree in electrical and computer engineering from the University Nova of Lisbon, Lisbon, Portugal, in 2017.

He is currently an Assistant Professor with the Universidade Lusófona, Lisbon. He is one of the winners of the fourth edition Scientific Employment Stimulus (CEEC Individual 2021) funded by Fundação para a Ciência e a Tecnologia. According to the methodology proposed by Stanford University, Stanford, CA, USA, he was among the most influential researchers in the world in 2019 and 2020, when he joined the list of top 2% of scientists whose work is most cited by other colleagues in the field of Information and Communication Technologies, sub-area Networks and Telecommunications. His research interests include target localization in wireless sensor networks, nonlinear, and convex optimization.

Muhammad Salman received the B.S. degree in electronic engineering from the Balochistan University of Information Technology, Engineering and Management Sciences (BUITEMS), Quetta, Pakistan, in 2010, the M.S. degree in electronic engineering from Politecnico di Torino, Turin, Italy, in 2014, and the Ph.D. degree in electrical and computer engineering from Inha University, Incheon, South Korea, in 2023.

From October 2014 to June 2019, he worked as a Lecturer with the Electrical and Computer Engineering Department, Effat University, Jeddah, Saudi Arabia. Currently, he is a Postdoctoral Researcher with the Korean Institute of Energy and Technology (KENTECH), Naju, Republic of Korea. His research interests include spy camera detection, bufferbloat mitigation, wireless networks, vital signs detection on mmWave, and software defined networks.

Youngtae Noh (Member, IEEE) received the B.S. degree in computer science from Chosun University, Gwangju, South Korea, in 2005, the M.S. degree in information and communication from the Gwangju Institute of Science Technology (GIST), Gwangju, in 2007, and the Ph.D. degree in computer science from the University of California at Los Angeles (UCLA), Los Angeles, CA, USA, in 2012.

He is an Associate Professor with the Energy AI, Korean Institute of Energy and Technology (KENTECH), Naju, Republic of Korea. Before joining KENTECH, he worked as an Associate Professor at Inha University Incheon, Incheon, South Korea, from 2015 to 2022. Moreover, he also worked at Cisco Systems, Milpitas, San Jose, CA, USA, as a Staff Member, from 2012 to 2014. His research interests include mobile/pervasive computing, mobile systems, mobile data science, mobile-HCI, cloud computing, data center networking, wireless networking, and future Internet.

Kiseon Kim (Life Senior Member, IEEE) received the B.Eng. and M.Eng. degrees in electronics engineering from Seoul National University, Seoul, Republic of Korea, in 1978 and 1980, respectively, and the Ph.D. degree in electrical engineering systems from the University of Southern California, Los Angeles, CA, USA, in 1987.

From 1988 to 1991, he was with Schlumberger, Houston, TX, USA. From 1991 to 1994, he was with the Superconducting Super Collider Laboratory, Waxahachie, TX, USA. In 1994, he joined Gwangju Institute of Science and Technology, Gwangju, Republic of Korea, where he is currently a Professor. His research interests include wideband digital communications system design, sensor network design, analysis and implementation both at the physical and at the resource management layers, and biomedical application design.

Dr. Kim is a member of the National Academy of Engineering of Korea, a Fellow of the IET, and a Senior Editor of the IEEE SENSORS JOURNAL.